Ultra-fast all-optical wavelength conversion in silicon waveguides using femtosecond pulses

R.Dekker[a], J. Niehusmann[b], M. Först[b], and A. Driessen[a]

[a] Integrated Optical Micro Systems, Mesa+, University of Twente, P.O. Box 217, 7500 AE Enschede, The Netherlands. Phone: +31-53-489 4440; E-mail: R.Dekker@utwente.nl.
[b] RWTH Aachen University, Institut für Halbleitertechnik, 52074 Aachen, Germany.

In this work, the propagation of 300 femtosecond optical pulses in Silicon-on Insulator waveguides has been studied by means of a pump-probe set-up. Large Cross Phase Modulation (XPM) induced red and blue shifts (9nm and 15nm, respectively) of the probe signal have been observed depending on the delay between pump (1554nm) and probe (1683nm) pulses. A numerical model taking into account Two Photon Absorption (TPA) and Free Carrier Absorption (FCA) in the semiconductor waveguide is presented and provides good agreement with the experimental data. Our model reveals that the wavelength conversion is dominated by the instantaneous optical Kerr effect, enabling ultra-fast all-optical functionalities. Furthermore, the importance of waveguide dispersion on the wavelength conversion efficiency will be treated in the case of femtosecond pulses.

Introduction

Silicon photonics is receiving increasingly attention, especially because of its potential for integration with microelectronics (1). In recent years many new types of nonlinear active silicon-based photonic devices have been developed. Substantial progress has been achieved in the field of Raman amplification, in both continuous-wave (2) and pulsed pump-probe (3,4) experiments. Other nonlinear effects like two-photon absorption (TPA) (5), self-phase modulation (SPM) (6,7), cross-phase modulation (XPM) and continuum generation (8), four-wave mixing (FWM) (9) and the Kerr coefficient (10) have been successfully demonstrated and thoroughly investigated.

In this paper, we present both theoretical and experimental results of femtosecond pump-probe experiments in Silicon-on-Insulator (SOI) waveguides. Large Kerr-induced wavelength shifts of the probe signal have been observed, whereas the free carrier contribution did not substantially contribute. Since the ultra-fast Kerr effect is the dominating mechanism, this method of wavelength conversion is suitable for ultra-fast all-optical switching. Finally, the importance of waveguide dispersion on the conversion efficiency will be discussed

Experimental setup

Figure 1 shows a schematic representation of our experimental setup. Both the pump (1554nm) and probe (1683nm) pulses with a FWHM pulse duration of 300fs are generated using an optical parametric oscillator (OPO), while their beam shapes are being modified by optical beam formers (OBF) in order to optimize the fiber coupling

efficiency. The time delay between pump and probe pulses is controlled with an optical delay line (ODL) with 6 femtosecond accuracy. Both beams are combined using a beam splitter (BS), polarized (Pol) and coupled into a 10cm piece of polarization maintaining fiber (PMF) using a microscope objective (MO). The output of the PMF is used to couple TM polarized light pulses into our SOI waveguides that have a 450nm×300nm (w×h) cross section (by design) and a length of 7mm. The transmitted pulses are coupled out using a single mode fiber, which is attached to an optical spectrum analyzer (OSA). Folding mirrors (FM) are used to tap the pump and probe signals to detect their power levels using an optical detector (OD). The pump intensity can be controlled using a neutral density filter (FW).

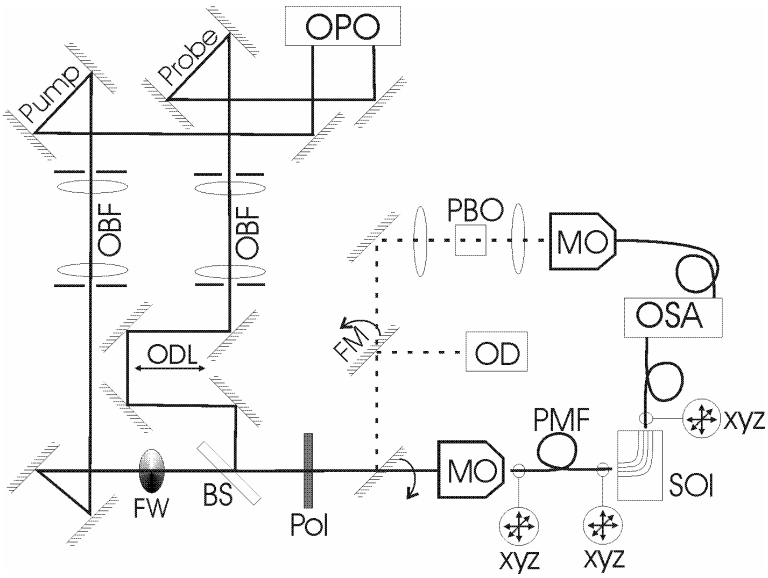

Figure 1. Schematic representation of the femtosecond pump-probe setup used in the experiments.

Theory

When strong pump pulses (I_{max}~10TW/m^2) propagate through a SOI waveguide, the refractive index of the material is changed mainly by two nonlinear effects. The first one is the instantaneous Kerr effect, inducing an ultra-fast refractive index increase of (10):

$$\Delta n_{Kerr}(t) = n_2 . I(t) \qquad [1]$$

Secondly, by TPA, free carriers (FCs) are generated that cause a refractive index decrease according to [4]:

$$\Delta n_{FC}(t) = -(8.8 \cdot 10^{-22} N(t) + 8.5 \cdot 10^{-18} N(t)^{0.8}) \qquad [2]$$

with N the free carrier density. Since both refractive index changes are intensity dependent, they both change with the envelope of the pulse and induce a temporal phase shift:

$$\Delta\phi(t) = \frac{2\pi L \Delta n(t)}{\lambda} \quad [3]$$

Here, L is the interaction length of pump and probe pulses. Consequently, this temporal phase shift causes a frequency shift $\Delta\omega(t)=d\Delta\phi(t)/dt$, which is the basis for SPM and cross phase modulation (XPM). In turn, the frequency shift causes the wavelength to shift, according to:

$$\lambda_s = \frac{\lambda_0}{1 - \frac{L_{\text{int}}}{c} \cdot \frac{\Delta n(t)}{dt}} \quad [4]$$

with λ_s the center wavelength of the frequency converted probe pulse, λ_0 the center wavelength of the original probe spectrum and c is the speed of light in vacuum. The intensity of the pulse and the amount of generated free carriers as function of the propagation distance of the pulse in the SOI waveguide can be calculated by numerically solving the following set of coupled differential equations (3):

$$\frac{dI(t,z)}{dz} = -\alpha I(t,z) - \beta I^2(t,z) - \sigma N(t,z) I(t,z) \quad [5]$$

$$\frac{dN(t,z)}{dt} = \frac{\beta}{2h\nu} I^2(t,z) - \frac{N(t,z)}{\tau} \quad [6]$$

where α is the linear absorption, β is the two photon absorption coefficient and σ is the free carrier absorption cross section, $h\nu$ the photon energy and τ the free carrier lifetime.

TABLE I. Overview of values used in the numerical simulations

Property	Symbol	Value
Waveguide cross section	w×h	450×300nm
Mode area	A_{eff}	~0.15μm^2
Waveguide length	L	7mm
Free Carrier lifetime	τ	5ns
Peak intensity	I_{max}	~10TW/m^2
Pulse repetition rate	F_{rep}	80MHz
Center wavelength of the pump	λ_p	1554nm
Center wavelength of the probe signal	λ_s	1683nm
linear absorption	α	0m^{-1}
TPA coefficient	β	5·10^{-12}m/W
free carrier absorption cross section	σ	1.45·10^{-21}·(λ/1.55) m^2
Kerr nonlinearity	n_2	4·10^{-18} m^2/W
Pulse shape	Gaussian	-

In Table II some numerical results of Equations [1-6] are presented at several propagation distances using the parameters from Table I. It can be concluded from the first graph in Table II that the pulse intensity decreases mainly due to TPA, since the pulse keeps its Gaussian shape. This is in contrast to pulses with a longer pulse duration (> 1ps), where the trailing edge experiences stronger absorption due to the generated free carriers, distorting the pulse shape. It can also be seen in the third graph that the Kerr induced refractive index change is the dominant mechanism. Even though the intensities are very high, a relatively low amount of free carriers are generated since the pulses are very short.

TABLE II. Simulation results of 300fs pulse propagation in SOI waveguides

	Simulation results
Pulse shape:	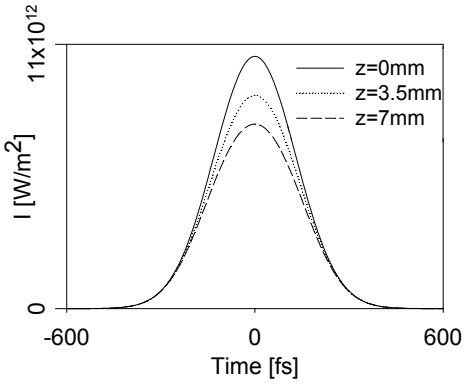
Free carrier density:	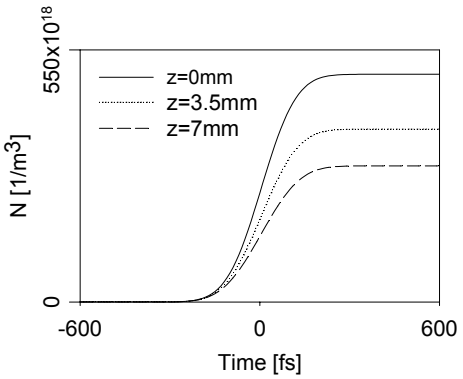
Refractive index change:	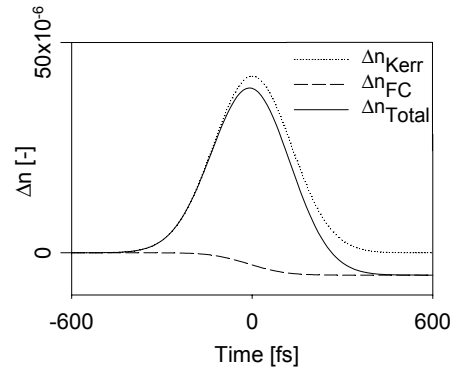
Wavelength shift:	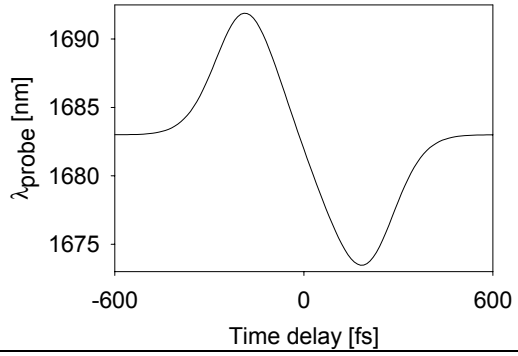

Experimental results

In Figure 2 the experimentally observed center wavelength of the probe pulses are plotted as function of delay time. Here a negative delay time means that the probe pulses are running ahead of the pump pulses, i.e. are overlapping with the leading edge of the pump pulse. The discrepancy between the experimental results and the simulations is caused by the fact that dispersion effects are not included in the previously discussed model. We observed a 10nm redshift at negative delay times, indicating that the nonlinearities are dominated by the Kerr effect in case of femtosecond pulses. This is in contrast to the blueshift that is normally observed in pump-probe experiments with longer ps pulses [1], where the free carrier dispersion effect is dominant due to the fact that ps pulses are long enough to build up a sufficient amount of free carriers.

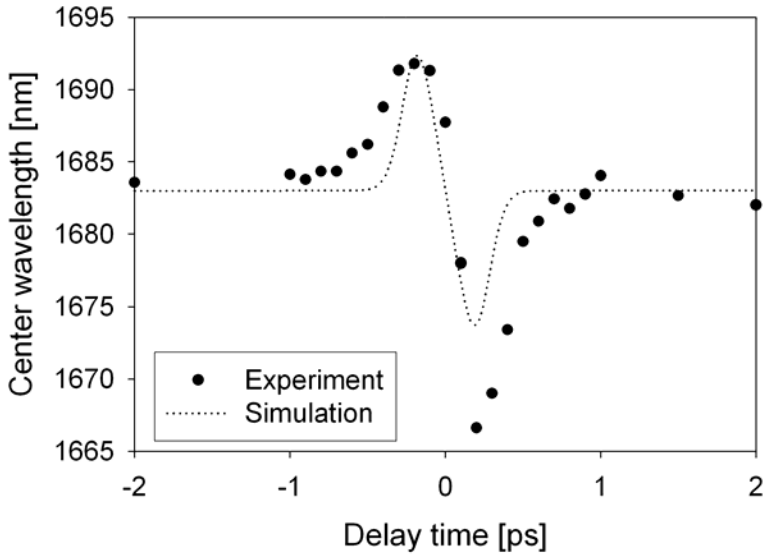

Figure 2: Center wavelength vs. delay time.

Waveguide dispersion

The geometry induced waveguide dispersion will dominate the material dispersion in case the SOI waveguide dimensions are in the submicron range [12]. The distance over which the pump and probe pulses pass through each other's envelope is called the walkoff length L_w and is defined as [12]:

$$L_w(\lambda) = T_0 \Big/ \left| \beta_{1p}(\lambda) - \beta_{1s}(\lambda) \right| \qquad [7]$$

where T_0 is the half width of the pulse, and β_{1p} and β_{1s} are the first order dispersion coefficients of the pump and probe, respectively. In Figure 3 the first order dispersion coefficients and walkoff lengths between the 1554nm pump and 1683nm probe pulses (T_0=300fs) are plotted for a SOI waveguide with a height of 300nm and the width as varying parameter. It can be seen that the waveguide width is a critical parameter that strongly affects the pump-probe interaction and therefore the maximum attainable wavelength conversion as the conversion efficiency increases with L_w.

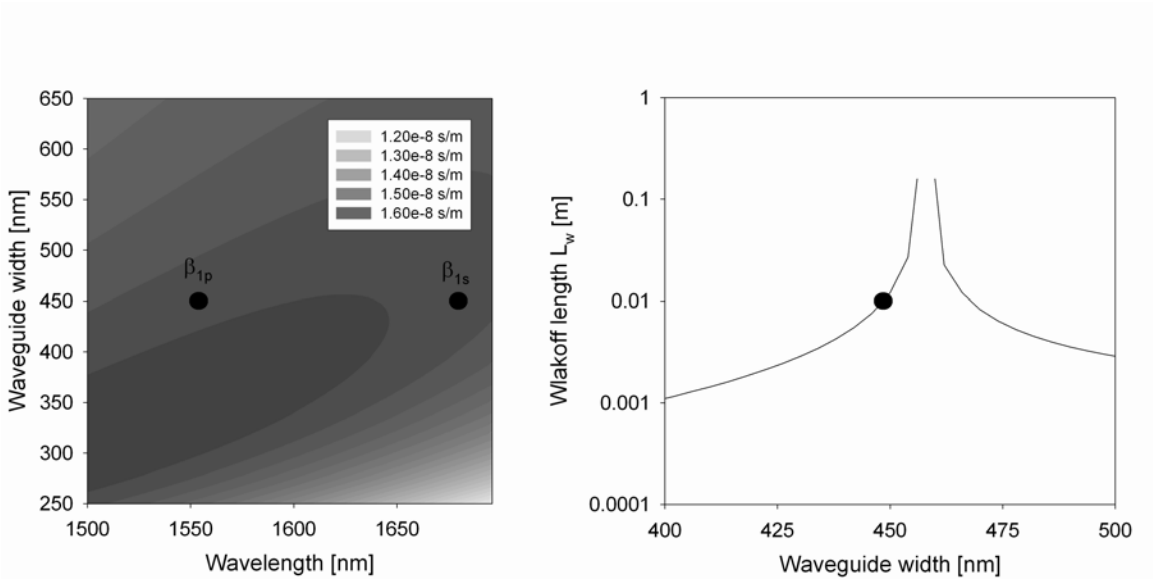

Figure 3: (left) First order dispersion β_1 as a function of wavelength and waveguide width. (right) Walkoff length vs. waveguide width.

To achieve efficient wavelength conversion, the pump and probe wavelengths need to be chosen such that both their first order dispersion values are on the same contour line, as can be seen in the left chart of Figure 3. The interaction length could easily be increased by increasing the pulse lengths, since the walkoff length scales linearly with the pulse length (see Equation [7]). However, at longer pulse lengths, the pulse envelope is less steep resulting in weaker wavelength conversion. The walkoff length can in principle go to infinity when the first order dispersion coefficients are exactly the same (right chart in Figure 3, around w=458nm). This ideal case can be achieved by tuning the pump and/or probe wavelengths or with extremely accurate control of the waveguide fabrication. We believe that the observed large wavelength shifts in short SOI waveguides can only be achieved with sub-picosecond pulses, combined with precise control of the waveguide dispersion.

Conclusions

We have shown that both 10nm blue and red shifts in SOI waveguides using a pump-probe setup with 300fs pulses are feasible. The XPM is dominated by the Kerr effect, since the pulses in the femtosecond regime are too short to accumulate a sufficient amount of free carriers to have considerable free carrier dispersion. This means that the temporal refractive index changes are mainly caused by the instantaneous Kerr effect and thus both the wavelength up and down-conversion takes place in a sub-picosecond timeframe. We have shown the importance of waveguide dispersion management on the wavelength conversion efficiency in femtosecond pump-probe experiments.

Acknowledgments

R. Dekker and A. Driessen would like to thank Freeband Impulse technology program of the Ministry of Economic Affairs of the Netherlands. All authors would like to acknowledge the European Network of Excellence on Photonic Integrated Components and Circuits (ePIXnet FAA5/WP11).

References

1. G. T. Reed, "Optical age of silicon", *Nature*, Vol **427**, 595-596, 2004.
2. V. Raghunathan, R. Claps, D. Dimitropoulos and B. Jalali, "Parametric Raman Wavelength Conversion in Scaled Silicon Waveguides", *J.Lightwave.Technol*, Vol **23** (6), pp 2094-2102, 2005.
3. A. Liu, H. Rong, M. Paniccia, O. Cohen and D. Hak, "Net optical gain in a low loss silicon-on-insulator waveguide by stimulated Raman scattering", *Opt.Express*, Vol **12** (18), pp 4261-4268, 2004.
4. Q. Xu, V. R. Almeida and M. Lipson, "Time-resolved study of Raman gain in highly confined silicon-on-insulator waveguides", *Opt.Express*, Vol **12** (19), pp 4437-4442, 2004.
5. T. K. Liang, H. K. Tsang, I. E. Day, J. Drake, A. P. Knights and M. Asghari, "Silicon waveguide two-photon absorption detector at 1.5μm wavelength for autocorrelation measurements", *Appl.Phys.Lett.*, Vol **84** (15), pp 2745-2747, 2002.
6. O. Boyraz, T. Indukuri and B. Jalali, "Self-phase-modulation induced spectral broadening in silicon waveguides", *Opt.Express*, Vol *12* (5), pp 829-834, 2004.
7. R. Dekker, E. J. Klein, J. Niehusmann, M. Först, F. Ondracek, J. Ctyroky, N. Usechak and A. Driessen, "Self Phase Modulation and Stimulated Raman Scattering due to High Power Femtosecond Pulse Propagation in Silicon-on-Insulator Waveguides." Symposium IEEE/LEOS Benelux Chapter, Mons, Belgium, pp 197-200, 2005.
8. O. Boyraz, P. Koonath, V. Raghunathan and B. Jalali, "All optical switching and continuum generation in silicon waveguides", *Opt.Express*, Vol **12** (17), pp 4094-4102, 2004.
9. H. Fukuda, K. Yamada, T. Shoji, M. Takahashi, T. Tsuchizawa, T. Watanabe, J. Takahashi and S. Itabashi, "Four-wave mixing in silicon wire waveguides", *Opt.Express*, Vol **13** (12), pp 4629-4637, 2005.
10. M. Dinu, F. Quochi and H. Garcia, "Third-order nonlinearities in silicon at telecom wavelengths", *Appl.Phys.Lett.*, Vol **82** (18), pp 2954-2956, 2003.
11. R. A. Soref and B. R. Bennett, "Electrooptical Effects in Silicon", *IEEE.J.Sel.Top.Quant.Electr.*, Vol **QE-23** (1), pp 123-129, 1987.
12. X. Chen, N. C. Panoiu and R.M.Jr.Osgood, "Theory of Raman-Mediated Pulsed Amplification in Silicon-Wire Waveguides", *IEEE J. Quant. Electr.*, Vol **42** (2), pp 160-170, 2006.